Double versus single junction: from tunneling to contact regime in a double quantum dot molecule system.

[a] Moreira, A.C.L* ; L. S. Marques [b]

[a] Núcleo Interdisciplinar em Ciências Exatas e da Natureza - NICEN
Universidade Federal de Pernambuco, 50740-540, Recife/PE, Brasil;

[b] Centro de Física das Universidades do Minho e do Porto,
Universidade do Minho, 4710-057, Braga, Portugal

*Corresponding author: aclm.ufpe@gmail.com

Abstract

In this work a theoretical study of the charge transport through a nanostructure composed by a double quantum dot was made by treating the system in two different ways: as single junction (SJ) within the scanning tunneling microscopy theory and a double junction (DJ) within the usual non equilibrium Green´s function theory approach. In the first case (SJ), the three blocks – contact-device-contact – is treated as a single junction by 'breaking' the nanostructure into two parts and considering each one as belonging to an 'extended contact'. In the DJ case, the usual treatment with two contacts-related broadening and the exact Green´s function describing the propagation inside the system was made. Proceeding in this way, for a minimum two-level model system, we show that the results obtained with the SJ and DJ treatment are identical despite they start with a different general formulae for transmission. Finally, both treatments were used with a minimal model for a biphenyl system in an asymmetric sample-biphenyl-tip configuration and analyzed in terms of a SJ point of view bringing another perspective to the main features of this system.

Keywords: A. Molecular Electronics.
D. Quantum transport.
D. STM-theory.

1. Introduction

Molecular electronics (ME) aims to develop devices to control the flow of electrons at nanoscale by using molecules as an active component [1-4]. For this, it is necessary to insert an organic component containing certain characteristics (asymmetry, for example) between two electrodes. Depending on the characteristics the molecule can function as an active component, allowing, for example, a greater flow of electrons in only one direction, such as in molecular transistors [5, 6]. Devices based on organic molecules, when compared to their silicon analogues, have several specific advantages, among which we can mention [7, 8]: size (molecules have nanometric dimensions and, therefore, ME devices may occupy much smaller volumes than current silicon-based components), speed (the time for an electron to pass through a molecule is faster than in silicon components) and functionality once on a nanometric scale, quantum effects such

as Coulomb blockade, among others, are present and can be used for the development of new types of devices.

From an experimental point of view, there are several methods fabricate a molecular device and measure its electrical properties, such as [4, 7]: the "self-assembly" sections (self assembly monolayer - SAM), a mechanically controlled junction break (MCBJ), an atomic force microscopy (AFM) and scanning tunneling microscopy (STM). In the latter, instead of a direct tip to tip coupling, a molecule can be attached between the tips and internal features of this compound (tips plus molecule) dictates how an electron propagates through it. Once a molecule is sandwiched between the tips, specific properties of the full system – geometrical structure, asymmetries, constrictions, vacancies and so on – will dictate the shape of electrical current of this system [6, 9]. When the strength of the interaction between the molecule and the metallic tips is large, we are in the so called strong coupling limit (sometimes referred to as the self-consistent field regime) where the molecular levels are broadened by their interaction with the contacts, resulting in a coherent (ballistic) electronic transport through the system [4, 10]. In this regime, perturbation theory is not valid anymore and the most used formalism, in this case, is the Landauer-Büttiker with an energy-dependent transmission probability function $T(E)$ calculated using Green´s function techniques [11, 12]. The device conductance obtained from transmission function is the key feature to determine charge transport properties through the nanostructure.

In this work we will study the charge transport through a nanostructure with two different approaches, here refereed as the single junction (SJ) and the double junction (DJ). For the SJ treatment, in spite of considering three blocks – contact-device-contact – we will 'break' the nanostructure in two parts, an extended right contact (containing part of the device), an extended left contact (containing the remaining part of the device) and use STM-theory of tunneling [2, 9, 13, 14] to study the electronic transport through these extended tips. The second approach we will use the standard Non Equilibrium Green´s Function (NEGF) treatment [11, 15, 16] for the transport in a double junction (DJ) system, consisting in three blocks – contact-device-contact. These two approaches, despite starting from a very distinct general expression for the transmission function, for a minimal two level model, give equal results. In what follows, we will describe the methodology of our theoretical approach in section 2 and in section 3 we will apply the described approach for a model composed by two sites connected within a tight binding model and present the main results. In section 4, we will use a DJ treatment to study the transport through a biphenyl molecule as function of the torsion angle and show how the results can be interpreted in terms of a SJ point of view. Finally, the conclusions and perspectives will be presented in section 5.

2. Eletronic transport methodology.

The electronic transport through a single molecule attached to two (*L*eft and *R*ight) electrodes will be treated as a single junction (SJ) problem within STM-theory approach and as a double junction (DJ) within NEGF and, for both methods we will calculate the transmission function for a minimal two level model. In principle, and for

different reasons, this problem could be viewed as a device connected to two electrodes forming a double junction or as two “extended-tips” with each part of the molecule forming an extended contact forming a single junction. For both cases, if a strong coupling limit exist, the strength of the interaction between the molecule and the metallic leads is large, resulting in a strongly hybridization between contacts and device (a molecule, for example) and the broadening of the device’s levels. In this limit, the transport is coherent and the Landauer approach can be used to describe the electronic transport through the molecule with the current calculated as [6, 10, 12]:

$$I = \frac{2e}{h}\int_{-\infty}^{+\infty} T(E)\big(f_L(E) - f_R(E)\big)dE \quad . \tag{1}$$

In Eq. (1) $f_L(E)$ { $f_R(E)$ } are the Fermi distribution functions of the left {right} electrodes and $T(E)$ is the total transmission function. This transmission, however, has different mathematical forms if we adopt a double junction (DJ) or a single junction (SJ) approach. In the DJ approach, a Non Equilibrium Green´s Function (NEGF) is used for the transmission in a linear regime and for a zero-temperature, which can be expressed as [10, 12]:

$$T(E) = Tr\left[\tilde{\Gamma}_L(E)\,\tilde{G}^{r}_{LR}(E)\,\tilde{\Gamma}_R(E)\,\tilde{G}^{a}_{LR}(E)\right] = Tr\left[\hat{t}(E).\hat{t}^{\dagger}(E)\right] \quad , \tag{2}$$

where

$$\hat{t}(E) = \tilde{\Gamma}_L^{1/2}(E)\tilde{G}^{a}_{LR}(E)\,\tilde{\Gamma}_R^{1/2}(E) \tag{3a}$$

$$\hat{t}^{\dagger}(E) = \tilde{\Gamma}_L^{1/2}(E)\tilde{G}^{r}_{LR}(E)\,\tilde{\Gamma}_R^{1/2}(E) \ . \tag{3b}$$

All quantities in brackets are matrices with dimension given by the number of elements of the atom-centered basis set spanning the system – usually an extended molecule with part of electrodes coupled at the ends – and *Tr* denotes the trace over the matrix. The terms $\tilde{\Gamma}_L$ and $\tilde{\Gamma}_R$ are the spectral matrix densities (the imaginary part of the self-energy) due to the coupling with left and right contacts and $\tilde{G}^{r/a}_{LR}$ is the retarded/advanced Green´s function which can be viewed as the probability for a particle to propagate along the device. We stress that only if $\tilde{\Gamma}_L$, $\tilde{\Gamma}_R$ and $\tilde{G}^{r/a}_{LR}$ are simultaneously diagonalizable, Eq. (2) can be reduced to a sum of independent eigenchannels contribution [17]: $T^{tot}(E) = \sum_{\alpha} T^{\alpha}(E)$.

For the SJ approach, the strong hybridization allow us represent each half of the system as the active part of an extended left tip/sample and an extended right tip/sample. The energy-dependent transmission consider the multiple scattering

processes at the junction, and in its matrix formulation the total contribution is given by the trace of the resultant matrix [2, 9, 14]:

$$T(E) = Tr\left[\hat{D}_L^r(E)\hat{V}_{LR}\, \hat{\rho}_{0R}(E)\, \hat{V}_{RL}\, \hat{D}_L^a(E)\, \hat{\rho}_{0L}(E) \right] = Tr\left[\hat{t}(E).\hat{t}^{\dagger}(E) \right] \quad , \tag{4}$$

where

$$\hat{t}^{\dagger}(E) = 2\pi\, \hat{\rho}_{0L}^{1/2}(E)\, \hat{V}_{LR} \hat{D}_R^r(E) \hat{\rho}_{0R}^{1/2}(E) \tag{5a}$$

$$\hat{t}(E) = 2\pi\, \hat{\rho}_{0L}^{1/2}(E)\, \hat{V}_{LR} \hat{D}_R^a(E) \hat{\rho}_{0R}^{1/2}(E) \tag{5b}$$

and

$$\hat{D}_L^{r/a} = \left(1 - \hat{G}_L^{(0)r/a}(E)\hat{V}_{LR}\, \hat{G}_R^{(0)r/a}(E)\hat{V}_{RL}\right)^{-1}. \tag{5c}$$

In previous equation, $\hat{\rho}_{0L}(E)$ $\{\hat{\rho}_{0R}(E)\}$ is the density of states for the independent left {right} contact, $\hat{G}_L^{(0)r/a}(E)\,\{\hat{G}_R^{(0)r/a}(E)\}$ the retarded/advanced Green´s function of the uncoupled left {right} tip and $\hat{V}_{LR}$ the coupling between left and right tips. We stress that another version for $\hat{t}(E)$, could be obtained by changing $L \rightarrow R$ (and $R \rightarrow L$) and using the identities: $\hat{V}_{LR}\hat{D}_R^{r/a} = \hat{D}_L^{r/a}\hat{V}_{LR}$ and $\hat{V}_{RL}\hat{D}_L^{r/a} = \hat{D}_R^{r/a}\hat{V}_{RL}$ [9, 14]. For a minimal two level model $(\varepsilon_a, \varepsilon_b)$ Eq. (5a) can be reduced into a simple and useful expression:

$$T^{ab}(E) = \frac{4\left[\pi\, \rho_{aL}(E)\right]\left[\pi\, \rho_{bR}(E)\right]\left|V_{LR}^{ab}\right|^2}{\left|1 - \hat{G}_{bR}^{(0)r}(E)\, \hat{G}_{aL}^{(0)r}(E)\left|V_{LR}^{ab}\right|^2\right|^2} \quad . \tag{6}$$

In what follows, we will apply both treatments (DJ → Eq. (2) and SJ → Eq. (4)) in a tight binding approach for a minimal two level model that consist in two sites each one connected to a semi-infinite lead and coupled with each other via a hopping term. At the end we will show that these two approaches are identical, allowing a SJ interpretation of DJ results and vice versa.

3. Two coupled sites in a tight binding model: theory.

To apply the SJ and DJ treatment, let´s consider a minimal model composed by two sites A and B, each one attached to a semi-infinite electrode as showed in figure 1(a).

Figure 1: (a) Model of two sites A and B connected to Left and Right semi-infinite electrodes and (b) the renormalized sites with the leads L [R] 'incorporated' in site A [B].

In previous figure, sites A and B represents the left and right moieties of a molecular system (such as an extended molecule composed by biphenyl connected to a small gold cluster, for example), with 'sites' L and R represents the Left and Right electrodes (or tips), respectively. The Hamiltonian of this system is given by:

$$\hat{H} = \hat{H}_D + \hat{H}_L + \hat{H}_R + \hat{V}_L + \hat{V}_R \tag{7a}$$

where:

$$\hat{H}_D = E_A \hat{c}_A^\dagger \hat{c}_A + E_B \hat{c}_B^\dagger \hat{c}_B + K\left(\hat{c}_B^\dagger \hat{c}_A + \hat{c}_A^\dagger \hat{c}_B\right) \tag{7b}$$

$$\hat{H}_L + \hat{H}_R = \sum_{l=1}^{\infty} E_l \hat{d}_l^\dagger \hat{d}_l + \sum_{r=1}^{\infty} E_r \hat{d}_r^\dagger \hat{d}_r \tag{7c}$$

$$\hat{V}_L + \hat{V}_R = \sum_l V_{Ll}\left(\hat{d}_l^\dagger \hat{c}_A + \hat{c}_A^\dagger \hat{d}_l\right) + \sum_r V_{Rr}\left(\hat{d}_r^\dagger \hat{c}_B + \hat{c}_B^\dagger \hat{d}_r\right) \quad . \tag{7d}$$

Note that there isn't a direct coupling between left and right electrodes, nor a direct coupling between left electrode [right electrode] and site B [A], thus all interactions are local. With an explicit matrix written, a decimation [18] procedure can be performed, resulting in renormalized energies in sites A and B, and an effective Hamiltonian for the system, as showed schematically in figure 1b. In the effective Hamiltonian, the site´s energies are renormalized and given, respectively, by: $\tilde{E}_A = E_A + \Sigma_L(E)$ and $\tilde{E}_B = E_B + \Sigma_R(E)$. The term $\Sigma_{L/R}(E)$ is the so called self energies and appears as a result of the coupling with semi-infinite leads and posses a real ($\Delta_{L/R}(E)$) and an imaginary part ($i\Gamma_{L/R}(E)$). While the real part shift the energies values the imaginary one broad the level given to it a finite life time. For simplicity, let´s employ the wide band limit approximation [19] where the self-energies are energy-independent and purely imaginary: $\Sigma_{L/R}(E) = i\Gamma_{L/R}$. With these considerations, for a simple two level model, the effective Hamiltonian can be written as:

$$\hat{H}^{eff} = \begin{pmatrix} E_A + i\Gamma_L & K \\ K & E_B + i\Gamma_R \end{pmatrix} \quad . \tag{8a}$$

Evidently that a matrix version exists and can be written as:

$$\hat{H}^{eff} = \begin{pmatrix} \hat{H}_A + i\hat{\Gamma}_L & \hat{K} \\ \hat{K} & \hat{H}_B + i\hat{\Gamma}_R \end{pmatrix} \quad , \tag{8b}$$

with all quantities ($\hat{K}, \hat{H}_{A/B}$ and $\hat{\Gamma}_{L/R}$) inside $\hat{H}^{eff}$ being subspace's matrixes. The transmission can now be obtained as:

i) DJ-theory: in this case the exact Green´s function can be easily obtained by its definition ($\hat{G}^r(E) = \left[E\hat{I} - \hat{H}^{eff} \right]^{-1}$, $\hat{I}$ is a 2x2 identity matrix) and given by:

$$G^r(E) = \frac{K}{(E - E_A - i\Gamma_L)(E - E_B - i\Gamma_R) - K^2} \quad . \tag{9}$$

The transmission is then given by:

$$T_{DJ}(E) = \frac{4\Gamma_L \Gamma_R K^2}{\left|(E - E_A - i\Gamma_L)(E - E_B - i\Gamma_R) - K^2\right|^2} \tag{10}$$

ii) SJ-theory: in this model the local density of states may be obtained by the usual relation [6, 20] $\pi \hat{\rho}_i(E) = -\operatorname{Im} \hat{G}_{ii}^{r\,(0)}(E)$ where the (0)-superscript means the Green´s function of the uncoupled renormalized sites. Thus we have:

$$\pi\hat{\rho}_{A/B}(E) = -\operatorname{Im} \hat{G}^{(0)}_{AA/BB}(E) = \frac{\Gamma_{L/R}}{\left[(E - E_{A/B})^2 + \Gamma_{L/R}^2 \right]} \quad . \tag{11}$$

Considering the real ($\operatorname{Re}\left\{ \hat{G}^{(0)r}_{L/R} \right\} = (E - E_{A/B}) \left[(E - E_{A/B})^2 + \Gamma_{L/R}^2 \right]^{-1}$) and imaginary parts of Green´s function in $\hat{D}_L^r$ (see Eq. (5d)), with $\hat{V}_{LR} = K$, the transmission is given by:

$$T_{SJ}(E) = \frac{4\Gamma_L \Gamma_R K^2 \, \Im(E)}{\left[(E - E_A)^2 + \Gamma_L^2 \right] \left[(E - E_B)^2 + \Gamma_R^2 \right]} \quad , \tag{12a}$$

where $\Im(E) = \left|1 + \Upsilon(E) + i\Lambda(E)\right|^{-2}$ with $\Upsilon(E)$ and $\Lambda(E)$ given by:

$$\Upsilon(E)=\frac{\left[\Gamma_L\Gamma_R-(E-E_A)(E-E_B)\right]K^2}{\left[(E-E_A)^2+\Gamma_L^2\right]\left[(E-E_B)^2+\Gamma_R^2\right]} \quad , \tag{12b}$$

$$\Lambda(E)=\frac{\left[\Gamma_L(E-E_B)+\Gamma_R(E-E_A)\right]K^2}{\left[(E-E_A)^2+\Gamma_L^2\right]\left[(E-E_B)^2+\Gamma_R^2\right]} \quad . \tag{12c}$$

Finally, with a little algebra, it's straightforward to show that with Eq. (12b-c), $\Im(E)$ can be written as:

$$\Im(E)=\frac{\left[(E-E_A)^2+\Gamma_L^2\right]\left[(E-E_B)^2+\Gamma_R^2\right]}{\left|(E-E_A-i\Gamma_L)(E-E_B-i\Gamma_R)-K^2\right|^2} \quad , \tag{12d}$$

which, substituting in Eq. (12a) recover, exactly, the DJ results as in Eq. (10). Thus, despite Eq. (2) and Eq. (4) have distinct starting points, both give the same final expression for the transmission. This fact allows different points of view when interpreting the same phenomenon. For the SJ case, broadening effects due to device-electrodes coupling appear naturally in the calculation of the local state density (LDOS), in the imaginary part of Green's function. Note that, while the Green´s function describes the propagation in each separate moiety, the STM theory 'solve' the scattering problem for a single barrier at some arbitrary point in the system (in our case, at the midpoint). The denominator of $\Im(E)$ takes into account multiple scattering processes (transmissions and reflection) summing infinite terms of a series expansion, thus converging to the exact solution. Note that the absence of $\Im(E)$ will result in an unsaturated tunneling current when the tip-sample distance becomes small.

For the DJ case, we have two scattering rates (barriers) at the junctions, with the Green´s function describing the propagation of a ´particle inside the full system, in our case, the two coupled sites. The strength of the coupling between electrodes also broad (and shift, if we discard the WBL approximation) the levels and all information of the full structure is contained in the exact Green´s function. Note that this is not true for the SJ case since this case involves the Green´s function for each separated site, i.e., in the absence of the internal coupling between them. However, the term $\hat{D}_L^r$ suppresses this lack, once it includes all orders of perturbation theory [13] so, correcting the Green´s function to its exact form. Note also, that for the DJ case, the net flux across the left junction and the net flux across the right junction are equal but with opposite sign if we are in a steady state situation where there is no net flux into or out of the device [10]. These different points of views are illustrated in figure 2.

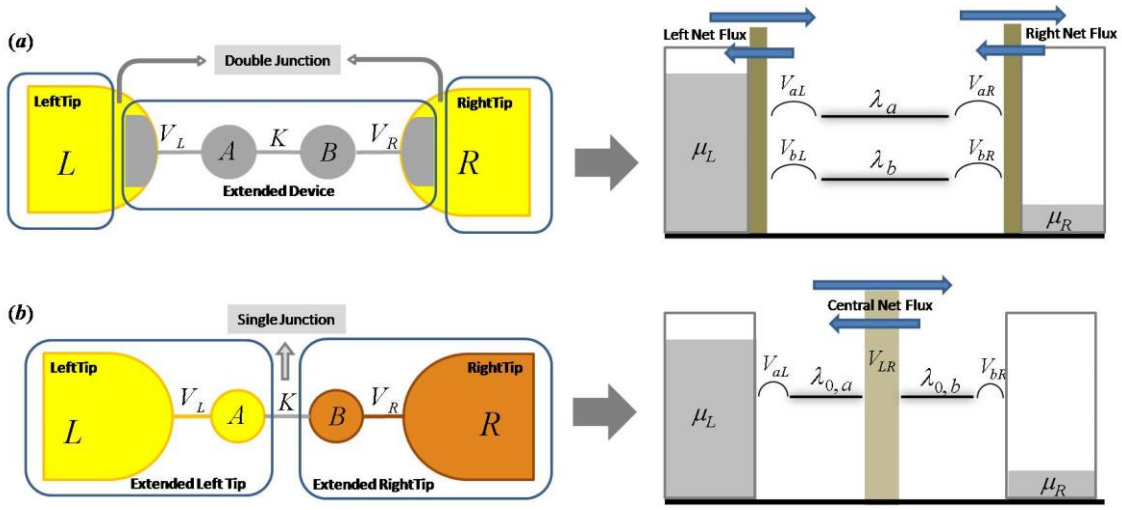

Figure 2: (a) DJ point of view formalism with part of the tips included in the system forming an extended device. (b) SJ-theory point of view of dealing with the same problem with the device as part of an extended tip.

In summary, the key feature of the similarity between both methods can be stated as follows: the point of the device where the electrical current is evaluated is somewhat arbitrary [6]. In other words, it doesn't matter if the electrical current is calculated at a single junction (SJ) or through double junction (DJ): for a given system the results must be independent of this choice, once at steady state there is no net flux into or out of the device [10]. This equivalence, allow us to use Eq. (10) instead of Eq. (12a) to address problems involving STM, since a full calculation of $\hat{D}_L^r$ using Eq. (12a) seems to be more cumbersome than the use of Eq. (10). We stress that the equality $T_{DJ}= T_{SJ}$ is valid even outside of WBL approximation. To see this, is enough to consider the full self energy correction adding the real part ($E_X \rightarrow E_X + \Delta_{X(E)}$) and the energy dependence in the broadening terms $\Gamma_X \rightarrow \Gamma_{X(E)}$ in Eq. (10) and Eq. (12a). In next section we will focus on understanding of how Eq. (10) can be interpreted in terms of the STM-theory.

4. Two coupled sites in a tight binding model: results.

The numerical parameters for the model system in fig 1, were conveniently chosen so as to consider an asymmetrical coupling ($(\Gamma_L ; \Gamma_R)=(0.16 ; 0.49)$), equal onsite energies (E_A=E_B=E_0=0) with the internal coupling between the sites (K) treated as a varying parameter assuming (in arbitrary units) the following values: K= 0.07, 0.15, 0.28, 0.50, 2.00 and 3.00.

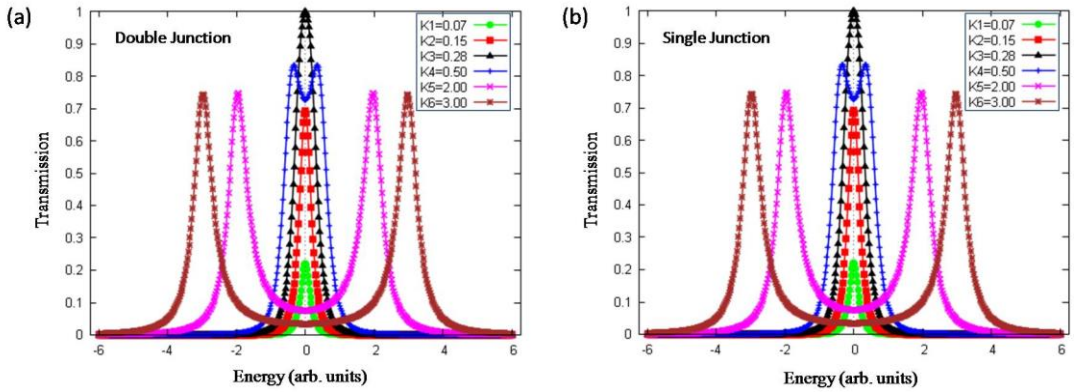

Figure 3: Transmission function for an asymmetric coupling (Γ_L = 0.16 and Γ_R = 0.49 – in arbitrary units) for different values of internal coupling *K:* (a) DJ approach. (b) SJ approach showing identical results for different formulas: Eq. (10) and Eq. (12a-c).

As shown in figure 3a-b) the transmission results are equal for both cases SJ and DJ approaches. The maximum peak in the transmission around $E=E_0$ is T=1 and occurs when $K = \sqrt{\Gamma_L.\Gamma_R} = K_C$, i.e., when K is equal to the geometric mean of the couplings – in our case, for K_C=0.28. As a consequence, for a symmetric coupling (where $\Gamma_R = \Gamma_L = \Gamma$) we have T=1 only when $K = \Gamma$, in accordance with the others works [21, 22]. Thus, the maximum value in transmission allow us to distinguish two 'regimes' relating $|K|$ and the coupling parameters: $K > \sqrt{\Gamma_L.\Gamma_R} = K_C$ and $K \leq \sqrt{\Gamma_L.\Gamma_R} = K_C$. When $K > K_C$, we are in the so called contact regime. In this case, the split of the two levels starts to become apparent as presented in figure 2, and despite the height of the curves, the area under the curves decreases around the fermi energy level and consequently the contribution for the electrical current decreases, reaching their maximum value for $K \gg \Gamma_L, \Gamma_R$. We stress that if the values of the coupling parameters ($\Gamma_{L/R}$) are very small, the contact regime is also called weak coupling limit. In this limit ($K \gg \Gamma_L \gg \Gamma_R$) the molecular levels are clearly resolved with a pronounced pseudo-gap between them and, consequently, we have two well defined eigenchannels with the transmission given by the Breit-Wigner formula as showed by magenta/x-letter and brown/asterisk curves in figure 3. Thus, the internal coupling for $K>K_C$ acts more as a measure of peaks distance ($d_{peaks}=2K$) between two Lorentzians curves than as a barrier inside the system. In this regime the system is almost transparent to the internal coupling [21-23], with the width fully 'controlled' by the coupling parameters ($\Gamma_{L/R}$), and the transmission through the system described by the Breit-Wigner formula for two independent eigenchannels.

The behavior of the transmission changes when $K \leq K_C$. In this case K acts like a internal 'barrier' in the sense that increasing its value the transmission´s peak also increases as shown in figure 3. Evidently that K is not only a 'barrier', but as mentioned before, it also splits the values of E_0 into two values ($E_0 \pm K$). As long as $K \leq K_C$, this effect is suppressed by the broadening effects, with the gap between $E_0 \pm K$ filled with states, which results in a non null transmission around the unperturbed level and with E_0 behaving like an 'effective' eigenchannel. We stress that near this limit (specifically

for $K \leq K_C / 2$) the tunneling approximation still works and an expression for the behavior in the tunneling regime can be obtained considering K<<1 in Eq. (12a) (or in Eq. (10)). In the both cases (SJ and DJ approaches), assuming that $\hat{D}_L^r \approx 1$, it's straightforward to show that Eq. (10) (or Eq. (12a)) can be approximated to:

$$T_{SJ/DJ}(E) \approx \frac{4\Gamma_L \Gamma_R K^2}{\left[(E-E_A)^2+\Gamma_L^2\right]\left[(E-E_B)^2+\Gamma_R^2\right]} = 4\pi^2 \rho_A(E)\rho_B(E)K^2 \quad . \qquad (13)$$

In figure 4 we plot the equation 13 and the exact solution for the transmission.

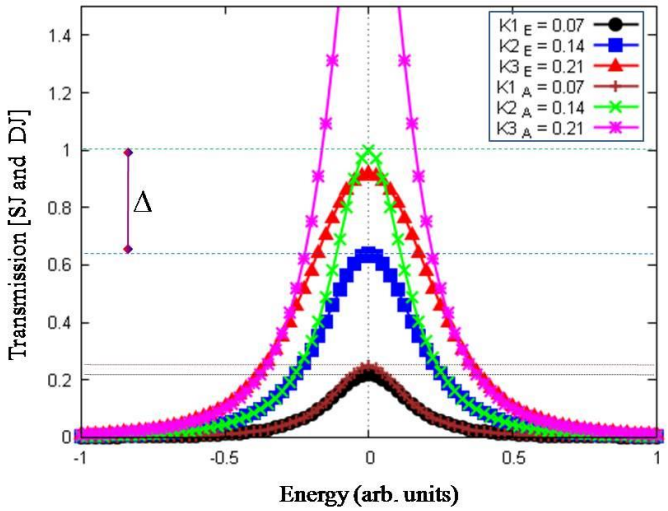

Figure 4: Transmission in the tunneling approximation (Eq. (13)) for different values of the internal coupling Kx$_A$ (x = 1, 2 and 3) and the exact solution (Eq. (10)) for different values of the internal coupling Kx$_E$ (x = 1, 2 and 3). Doted and Dashed lines indicates the difference between the approximated and the exact height of peaks for the pairs (K1$_E$; K1$_A$) and (K2$_E$; K2$_A$).

As expected for small values of K, the exact (Eq. (10)) and the approximated solution (Eq. (13)) almost coincide (see doted lines in figure 4). But increasing K, the peaks of the approximated solution grow up quicker than the exact solution. Note that for the resonance (E= E_0), when $2K = \sqrt{\Gamma_L.\Gamma_R} = K_C$, the approximate transmission is one and after this value, the transmission peaks blow up as depicted in the blue curve of figure 4. However, it remains finite and lower than one for the exact solution for all transmission peaks as shown in figure 4, by the dark-blue/x-points curve. Thus, in principle, despite overestimate the peak's height, K_C/2 defines the limit – in the sense that its maximum value is T=1 – of the tunneling regime and consequently, the application of the approximation in Eq. (13). Because this critical value is related to the couplings parameters $\Gamma_{L/R}$, we can see that for situations where there is a strong coupling between just one side of the SJ (left tip, for example) and the system and a very weak coupling between the system and the other tip, Eq. (13) fails. In particular, when $\Gamma_L >> \Gamma_R$ with $\Gamma_R \rightarrow 0$ (or vice-versa) due to the strong asymmetry, the tunneling limit becomes too restrictive since in this case $K_C \rightarrow 0$.

5. Tight Binding (TB) and Double Two Level Model (DTLM) approach for biphenyl

In previous section it was discussed the transition between tunneling and contact regimes in quantum transport for a two level model system. For some reason, this type of analysis is also usually made in a STM-theory context where the tip-sample distance defines the transport regime: while a small distance implies in a strong coupling parameter between tip and sample and configures a contact regime, a long distance is related to a weak coupling parameter and configures a tunneling regime. But if, instead a direct coupling between the tip and the sample, we have a quantum circuit between them (a molecule, for example), the internal structure of the device can define the transport regime even for a small tip-device distance. A well known example of an internal parameter that may define the transport regime is the torsion angle (φ) in a biphenyl molecule [22-24]: the coupling between the two rings can be drastically reduced when the torsion angle between them, goes from 0 to 90 degrees [21-23]. This behavior can change the transport regime and, motivated by this peculiarity, we will apply both approaches (DJ and SJ) to study the quantum transport transition regime through this system. For this, we opt for a system disposed in an asymmetric configuration (tip-device-sample), and the transmission calculated by different methods: a Tight Binding (TB) approach within the DJ theory (DJTB), a Tight Binding with the SJ theory (SJTB) and a Double Two Level Model (DTLM) with the transmission as defined by Eq. (10).

As mentioned above, the biphenyl system in figure 5a, changes its conductance as function of the torsion angle between the rings. This fact occurs even for small distances between the tip and the molecule. Experiments with STM-break junction technique show that the conductance can vary drastically depending if the rings are in a planar or in a perpendicular conformation, the latest one showing a tunneling like regime. The change in conductance from contact to tunneling regime reported by these experiments suggests that the conductance depends on the internal torsion angle and obeys a $cos^2(\varphi)$ law [22, 23].

From a theoretical point of view, the minimal model that can be used to explain this result is a ‘two level model’ (TLM) approach [21, 22] or a four level model (FLM) approach [25]. In these models the on-site parameters are the pair's energies of some frontier molecular orbital (highest occupied molecular orbital - HOMO or the lowest unoccupied molecular orbital - LUMO) for each separated moiety (see fig. 5b). Their energy values are usually obtained: either by fitting experimental results [22] or they can be parameterized by other reference theoretical methods such as density functional theory (DFT) or a simple tight binding approach (TB). Finally, with all necessary parameters in hand, the cosine law can be applied for subsequent calculations.

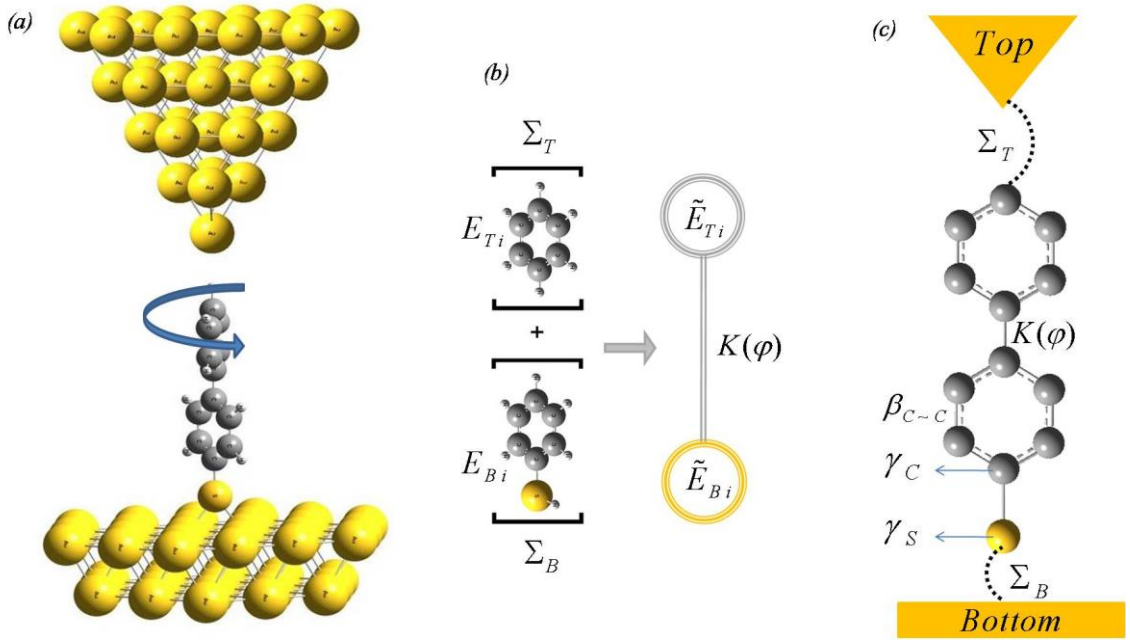

Figure 5: (a) Schematic view of a biphenyl coupled to gold atoms via sulfur 'clips'. (b) Two level model where each phenyl ring is treated as a site and each degenerate state as channels in parallel with a coupling proportional to *cos(φ)*. In (c) the 'geometry' for obtain the parameters for a two level model. The torsion angle *φ* represented in panel (d).

In this work we choose to compare between the transmissions obtained with DJTB and SJTB approaches with an alternative treatment: a DTLM model as defined by Eq. (10). Employing the wide band limit approximation [8, 20, 26], the effective Hamiltonian can be constructed as follows:

i) DJTB - in this case (see figure 5c) the molecular Hamiltonian contains five parameters: the on-site parameters for sulfur and carbons (γ_C and γ_S), the carbon-carbon and sulfur-carbon interaction ($\beta_{C\sim C}$ and β_{SC}) and the Top (T) and Bottom (B) line broadening matrix Γ_X ($X = T, B$). As usual [27-29] a simple formulae for the parameters can be adopted, denoting by $\gamma_X = \gamma + a_X \beta$ and $\beta_{XY} = b_{XY} \beta$, the on-site energy at the X-atom and the resonance integral between atoms X and Y, respectively. Conventionally [6, 27, 28], γ is taken as the $2p_x$-orbital energy of carbon and β the resonance bond integral – represented by tilde between carbons (C~C) to differentiate single (C−C), double (C=C) and triple (C≡C) bond – between the $2p_x$-orbitals of adjacent carbons with values given by $\gamma = \gamma_C = 0$ and $\beta = \beta_{C\sim C} = 1$. Thus, all energies are measured in units of resonance integral with the on-site parameter of carbon taken as the zero level. For the sulfur on-site energy and the intra-site coupling energy we use [27] $a_S = 0.43$ and $b_{SC} = 0.8$, respectively, and the single bond between the phenyl rings we have $b_{C\text{-}C} = 0.9$ which result in an inter-ring coupling given by: $K(\varphi) = 0.9 \cos(\varphi)$. For the coupling between the molecule and the semi-infinity systems (Tip and Sample), we employ the wide band limit approximation and assume that the tip (T) and sample (B) self-energies matrices are non null only at the terminal carbon and at the sulfur atom as showed in figure 5c.

Also, to simulate the asymmetry between the sample at the Bottom (strongly coupled) and the tip (weakly coupled) we take Γ_B = 1 *eV* >> Γ_T = 0.01 *eV*. Finally, we solve the pair of non-hermitian Hamiltonian [30, 31],

$$\left(H_0 + i\Gamma_T + i\Gamma_B\right)\Phi_k = \lambda_k \Phi_k \tag{14a}$$

$$\left(H_0 - i\Gamma_T - i\Gamma_B\right)\Psi_k = \lambda_k^* \Psi_k \ , \tag{14b}$$

`

which satisfy the bi-orthonormal relation [30] $\langle \Phi_k | \Psi_l \rangle = \delta_{k,l}$ and allow us to write the Green´s function into a spectral form:

$$G_{n,m}^r = \sum_k \frac{\phi_{m,k}\, \psi_{n,k}^*}{\lambda - \lambda_k} \, . \tag{15}$$

In Eq. (15) $\phi_{m,k}$ and $\psi_{m,k}$ are the expansion (complex) coefficients of the linear combination of atomic orbitals (LCAO) of Φ_k and Ψ_k, respectively. Notice that H_0 in Eqs. 14a-b is related to the full system: left and right phenyl rings.

ii) SJTB –At first we solve the pair of effective top moiety (*X* = *T*, *x* = *t*) and the effective bottom moiety (*X* = *B*, *x* = *b*), separated:

$$\left(H_{0,X} + i\Gamma_X\right)\Phi_x = \lambda_x \Phi_x \tag{16a}$$

$$\left(H_{0,X} - i\Gamma_X\right)\Psi_x = \lambda_x^* \Psi_x \ , \tag{16b}$$

that again satisfy the bi-orthonormal relation [30] $\langle \Phi_k | \Psi_l \rangle = \delta_{k,l}$ and allow us to write the (*n;m*)-element of the retarded Green's function ($G_{x,n,m}^{(0)\,r}$) for each separated (unperturbed) moiety in its spectral form:

$$G_{x,n,m}^{(0)\,r} = \sum_x \frac{\phi_{m,x}\, \psi_{n,x}^*}{\lambda - \lambda_x} \, . \tag{17}$$

Again, $\phi_{m,x}$ and $\psi_{m,x}$ in Eq. (17) are the expansion (complex) coefficients of the linear combination of atomic orbitals (LCAO) of Φ_x and Ψ_x, respectively. Once we have the Green´s function, the density matrix for each moiety ($\hat{\rho}_X$, *X* = *T*, *B*) can be obtained by Eq. 11. Note that so far, we obtained the operators (effective Hamiltonian, Green´s function, density matrix) for each separate moiety that is nothing but a subspace of the full system, the latter given by the direct sum of each subspace. Thus, for a given

operator ($\hat{O}$) we have: $\hat{O}_{Full} = \hat{O}_T \oplus \hat{O}_B$, and in the full space, each moiety operator is just the projection into a specific subspace. The full Green´s function, for example, is:

$$\hat{G}^{(0)r} = \begin{pmatrix} \hat{G}_T^{(0)r} & \hat{0} \\ \hat{0} & \hat{G}_B^{(0)r} \end{pmatrix} \quad , \tag{18}$$

and

$$\hat{G}_T^{(0)r} = \hat{P}_T \hat{G}^{(0)r} = \begin{pmatrix} \hat{G}_T^{(0)r} & \hat{0} \\ \hat{0} & \hat{0} \end{pmatrix} \quad . \tag{19}$$

Finally, defining $\hat{V}$ as:

$$\hat{V} = \begin{pmatrix} \hat{0} & \hat{V}_{TB} \\ \hat{V}_{TB} & \hat{0} \end{pmatrix} \quad , \tag{20}$$

we can apply Eq. 4 and obtain the transmission function for the SJ case within the STM-theory.

iii) DTLM – in this model the on-site parameters are the pair's energies of the HOMOs and LUMOs of each separated moiety. The effective Hamiltonian is a 4x4 block matrix, composed by a direct sum of (non interactive) HOMO subspaces and LUMO subspaces ($\hat{H}_{TOT}^{eff} = \hat{H}_{HOMOs}^{eff} \oplus \hat{H}_{LUMOs}^{eff}$), with each block given by:

$$\hat{H}_y^{eff} = \begin{pmatrix} E_{Ty} + i\Gamma_T & K(\varphi) \\ K(\varphi) & E_{By} + i\Gamma_B \end{pmatrix} \quad , \quad y = HOMO \, , \, LUMO \quad . \tag{15}$$

The parameters of the DTLM were obtained from the DJTB results. More specifically, while the inter-site coupling and the on-site energy were chosen so as to fit the real part of HOMO-1, HOMO, LUMO and LUMO+1 of the DJTB eigenvalues, the level broadening are chosen to fit the order of magnitude of the transmission peaks and such that $\Gamma_B >> \Gamma_T$. Proceeding in this manner and remembering that $K(\varphi) = K_0.cos(\varphi)$, we have: ($E_{T,HOMO}$, $E_{B,HOMO}$, $E_{T,LUMO}$, $E_{B,LUMO}$, K_0) = (*-1.0* , *-1.1* , *1.0* , *1.2* , *0.3*), Γ_B = 0.1 and Γ_T = 0.005, all quantities in *eV*. The transmission functions are shown in figure 6a-d for three different values of torsion angle (10°, 40° and 70°).

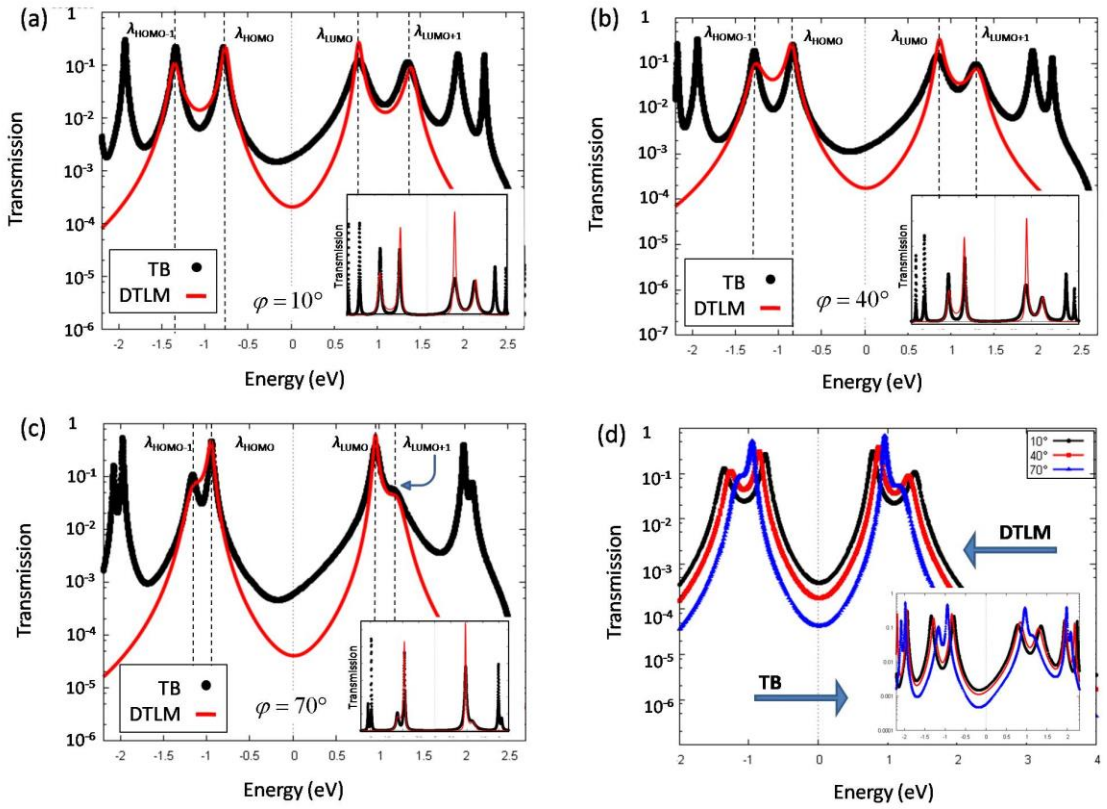

Figure 6: Transmission function for biphenyl within DTLM (red/line) and TB (DJ and SJ) (black line/circle) approaches: (*a*) for φ=10°, (b) φ=40° and (c) for φ=70°. In (d) we put for all DTLM results (for the three torsion angles) together and for TB approach in the inset.

Notice that, as for the simple TLM, the TB approach giveidentical results for DJ (eq 2) and SJ methods (Eq. 4). The same treatment must be used to incorporate the semi-infinity contacts and in our case, we opt for a simple WBL approximation. Therefore, with this in mind, from now on we will consider the DJTB and SJTB approaches as TB in general.

Observing figures 6a-c, the DTLM gives a good description of the two first unoccupied and occupied levels, when comparing with the TB approach. Around E=0 the energy positions of the four peaks in the transmission function, not only coincides (as expected) but, once the DTLM parameters ($E_{X,Y}$, K_0, Γ_X) were fixed, they described the same trends as in TB: the splitting of unoccupied and occupied levels decrease when the torsion angle increases. On the other hand, in the HOMO-LUMO gap region, the DTLM approach underestimates the magnitude of the transmission when compared with the TB approach. This discrepancy is a result of the odd number of sites in the TB approach with a complex eigenvalue with a real part near E=0 having a very high imaginary part but with a small transmission's coefficient in the Green´s function. This feature is absent in DTLM treatment. However, as shown in Fig. 6(d), in both cases (TB and DTLM), outside the HOMO/HOMO-1 and LUMO/LUMO+1 gaps, we have $T_{10°} > T_{40°} > T_{70°}$, showing that the smaller the torsion angle, the greater the conductivity of the system[22, 24, 26]. The same is not valid inside the gap, since increasing the torsion angle the HOMO/HOMO-1 peaks becomes closer, thus summing their intensities and resulting in higher transmission in the gap region. The same behavior is also observed for LUMO/LUMO+1 peaks. We stress that this peculiar aspect is not enough to change

the global behavior of the conductance, since the electrical current involves an integration over de energy within the Fermi window where, in general, we have $T_{10°} > T_{40°} > T_{70°}$. The DLTM approach could also be analyzed from a STM-theory point of view, focusing on the transport regime as function of the torsion angle. For φ=10° (see fig 6(a)) we can observe the splitting of the HOMO levels around E=-1.2 eV from their uncoupled values., which is related to the strong coupling of the phenyl rings due to the small torsion angle between them. In this case we have: $|K_{0\,(10°)}| = 0.295 > K_C = 0.023$, with the molecular levels being clearly resolved with a pronounced gap between them, resulting in two well defined eigenchannels in the transmission function. This can be viewed as a contact transport regime. The same reasoning can be applied for LUMO and LUMO+1 levels, around $E=1$ eV. This behavior is still valid for φ=40° where, in this case we have $|K_{0\,(40°)}| = 0.23$ eV $= 10K_C$, but with the gap between the peaks becoming smaller. However for large torsion angles φ=70°, the peaks become unresolved as as evident in Fig. 6(c). In this case we have $|K_{0\,(70°)}| = 0.1$ eV $\sim 4K_C$ and we can perceive a transition from the contact transport regime to the tunneling one. One might expect that above this value of torsion angle, the gap between these pair of levels decreases even further, with each pair of levels becoming a single effective transport channel and, in this case we are dealing with a tunneling transport regime.

Evidently that, by considering more levels, in principle, more peaks would appear, as one can see for the TB approach. However, the analysis is similar and this simple DLTM explains the essence of the physical behavior of this system within SJ point of view for a less cumbersome DJ transmission formulae.

6. Conclusions

In this work we study the transmission through a molecular system using a double junction (DJ) – and single junction (SJ) mathematical treatment. Employing the wide band limit for a minimal two level model (TLM), we develop two exact formulas for the transmission function: one starting from a STM-theory and treating the system as single junction and another one starting from the usual NEGF and treating the system as a double junction. Despite starting from different general formulae, we show that for a TLM the final results are similar, allowing us to choose the use of the least cumbersome one and interpret results in light of both points of view.

To illustrate the application of this equality between DJ and SJ-theory we apply both formulas to understand the transmission through an ideal double quantum dot asymmetrically attached to two semi-infinite systems, representing a typical STM device composed by a tip-device-sample configuration. In a second case study, we calculated the transmission in a biphenyl molecule connected between gold atoms, using a standard tight binding approach (DJTB and SJTB) and an alternative one here called double two level model (DTLM) approach. Within a wide band limit approximation, for both cases (DJ and SJ) an analytic expression was obtained and showed that the equality between the two treatments holds, also in a matrix form. Therefore, the results obtained within a DJTB treatment, can be interpreted in light of

the STM-theory (SJ) where a transition from tunneling regime to contact regime can be verified when the torsion angle between the rings decreases. Thus, while for the contact regime the split of the almost degenerate (unperturbed) levels gives rise to two well resolved channels for transmission, while for the tunneling regime each pair of levels becomes a single effective transport channel. Because the transition from one transport regime to another can occur even for a small distance, depending only of the torsion angle, the equality between DJ and SJ treatment enable us to use STM concepts for situations involving double junctions. Finally, we stress that despite the simple models adopted in this work, we showed that the equivalence between DJ and SJ-theory can be a valuable tool to study these systems, bringing new insights on the behavior of the system and permitting the use of a less cumbersome treatment for a given situation.

7. Acknowledgments

This research was carried out with financial support from Federal University of Pernambuco (Brazil). L. Marques acknowledges the financial support of the Portuguese Foundation for Science and Technology (FCT) in the framework of the Strategic Funding UIDB/04650/2020 and project SATRAP (POCI-01-0145-FEDER-028108).

8. References

1. Aviram, A. and M.A. Ratner, *Molecular Rectifiers.* Chemical Physics Letters, 1974. **29**(2): p. 277-283.
2. Vidal, F.J.G., F. Flores, and S.G. Davison, *Propagator theory of quantum-wire transmission.* Progress in Surface Science 2003. **74**: p. 8.
3. Remacle, F. and R.D. Levine, *Electrical transmission of molecular bridges.* Chemical Physics Letters, 2004. **383**(5-6): p. 537-543.
4. Lundstrom, M., *Nanoscale transistors: device physics, modeling and simulation.* 2006, New York: Springer.
5. Blanter, Y.V.N.a.Y.V.M., *Quantum Transport: Introduction to Nanoscience*. 2009, New York: Cambrige University Press.
6. Juan, E.S. and C. Cuevas, *Molecular Electronics: An Introduction to Theory and Experiment* Nanoscience and Nanotechnology, ed. M. Reed. Vol. 1. 2010: Word Scientific.
7. Durkan, C., *Current at the nanoscale: an introduction to nanoelectronics*. 2007, London: Imperial College Press; Distributed by World Scientific Pub. 211.
8. Xu, B. and Y. Dubi, *Negative differential conductance in molecular junctions: an overview of experiment and theory.* Journal of Physics: Condensed Matter, 2015. **27**: p. 19.
9. Blanco, J.M., F. Flores, and R. Pérez, *STM-theory: Image potential, chemistry and surface relaxation.* Progress in Surface Science, 2006. **81**: p. 41.
10. Datta, S., *Quantum transport: atom to transistor*. 2005, Cambridge, UK ; New York: Cambridge University Press. xiv, 404 p.

11. Datta, S., M.A. Ratner, and Y. Xue, *First-principles based matrix Green´s function approach to molecular electronic devices: general formalism* Chemical Physics, 2002. **281**: p. 20.
12. Di Ventra, M., *Electrical transport in nanoscale systems*. 2008, Cambridge: Cambridge University Press. xvi, 476 p.
13. Mingo, N., et al., *Theory of the scanning tunneling microscope: Xe on Ni and Al.* Physical Review B, 1996. **54**(3): p. 11.
14. Ferrer, J., A.M. Rodero, and F. Flores, *Contact resistance in the scannissg tunneling miscroscope at very small distances.* Physical Review B, 1988. **38**(14): p. 3.
15. Cuevas, J.C., et al., *Theoretical description of the electrical conduction in atomic and molecular junctions.* Nanotechnology 2003. **14**: p. 10.
16. Kopf, A. and P. Saalfrank, *Electron transport through molecules treated by LCAO-MO Green's functions with absorbing boundaries.* Chemical Physics Letters 2004. **386** p. 8.
17. Liu, Z.-F. and J.B. Neaton, *Energy-dependent resonance broadening in symmetric and asymmetric molecular junctions from an ab initio non-equilibrium Green's function approach* J. Chem. Phys., 2014. **141**: p. 5.
18. al, P.R.L.e., *Tuning the through-bond interaction in a twocentre problem.* Journal of Physics: Condensed Matter 1990. **2** p. 14.
19. Verzijl, C.J.O., J.S. Seldenthuis, and J.M. Thijssen, *Applicability of the wide-band limit in DFT-based molecular transport calculations.* The Journal of Chemical Physics, 2013. **138**: p. 11.
20. Ishida, H. and A. Liebsch, *Coulomb blockade and Kondo effect in the electronic structure of Hubbard molecules connected to metallic leads: A finite-temperature exact-diagonalization study.* Physical Review B, 2012. **86**: p. 13.
21. Pauly, F., et al., *Density-functional study of tilt-angle and temperature-dependent conductance in biphenyl dithiol single-molecule junctions.* Physical Review B, 2008. **77**: p. 9.
22. Mishchenko, A., et al., *Influence of Conformation on Conductance of Biphenyl-Dithiol Single-Molecule Contacts.* Nano Letters, 2010. **10**: p. 8.
23. Johansson, M.P. and J. Olsen, *Torsional Barriers and Equilibrium Angle of Biphenyl: Reconciling Theory with Experiment.* J. Chem. Theory Comput., 2008. **4**: p. 12.
24. Cohen, R., et al., *Charge Transport in Conjugated Aromatic Molecular Junctions: Molecular Conjugation and Molecule-Electrode Coupling.* J. Phys. Chem. C, 2007. **111**: p. 10.
25. Frisenda, R., et al., *Mechanically controlled quantum interference in individual π-stacked dimers.* Nature Chemistry, 2016. **8**: p. 6.
26. Bürkle, M., et al., *Conduction mechanisms in biphenyl dithiol single-molecule junctions.* Physical Review B, 2012. **85**: p. 12.
27. Baird, N.C. and A. Whitehead, *Coulomb Parameters in Simple Hückel and Omega Technique Molecular Orbital Methods* Canadian Journal of Chemistry, 1966. **41**: p. 11.

28. Yamada, H. and K. Iguchi, *Some Effective Tight-Binding Models for Electrons in DNA Conduction: A Review.* Advances in Condensed Matter Physics, 2010. **2010**: p. 28.
29. Zotti, L.A. and E. Leary, *Taming quantum interference in single molecule junctions: induction and resonance are key.* Phys.Chem.Chem.Phys., 2020. **22** p. 9.
30. Xie, H., et al., *Complex absorbing potential based Lorentzian fitting scheme and time dependent quantum transport.* The Journal of Chemical Physics 2014. **141**(164122): p. 14.
31. Cook, B.G., P. Dignard, and K. Varga, *Calculation of electron transport in multiterminal systems using complex absorbing potentials.* PHYSICAL REVIEW B 2011. **83**: p. 12.